The effect of Ni^{2+} substitution on $CoFe_2O_4$ based on natural iron sand using co-presipitation method

Nurmadina[1], P.L. Gareso[1*], N.S. Asri[2], A.P. Tetuko[2], E.A. Setiadi[2*]

[1]Departement of Physics, Faculty of Mathematics and Natural Sciences, Hasanuddin University, Jl. Perintis Kemerdekaan KM 10 Tamalanrea-Makassar 90245 Indonesia.

[2]Recearch Centre of Physics, Indonesia Institute of Sciences (LIPI), Puspiptek Area, Tangerang Selatan 15314, Indonesia.

[*] corresponding author : eko.arief.setiadi@lipi.go.id

ABSTRACT

Magnetic nanoparticles of Cobalt Nickel Ferrite ($Co_{1-x}Ni_xFe_2O_4$) have been synthesized by the co-precipitation method with various concentrations of moles of Ni^{2+} as a constituent in $Co_{1-x}Ni_xFe_2O_4$ (x = 0.25, 0.50 and 0.75). The $Co_{1-x}Ni_xFe_2O_4$ structured shows the single phase of crystal was formed with a cubic spinel structure. The crystallite size estimated using the Scherer formula was found that the crystallite size decreased with increasing concentration of Ni^{2+}. The samples with various concentration of Ni^{2+} showed coercivity and saturation magnetization was decreased by the increasing of concentration of Ni^{2+}.

Keywords: nanoparticles, $Co_{1-x}Ni_xFe_2O_4$, co-precipitation

1. INTRODUCTION

In recent years, the spinel ferrite nanoparticles are one of the most promising materials that were taken the interest of researchers for both scientific and technological applications due to it has unique magnetic, electrical, dielectric and optical properties. The spinel ferrite nanoparticles are includes in soft magnetic material with the structural formula MFe_2O_4 (where, M = two valence metal ions, for example, Mn, Mg, Zn, Ni, Co, and Cu) with cubic spinel crystal structure [1-2], for the distribution of ion $A^{3+}[B^{2+}B^{3+}]O_4^{2-}$ where A indicates the tetrahedral site and B represent the octahedral site. The A tetrahedral site is occupied by half the Fe^{3+} and the M^{2+} valence. The spinel ferrite (MFe_2O_4) also known to have good magnetic, optical, electrical, and dielectric properties at the nanoscale. The doping with selective elements suggests an effective method for enhances and controls these properties of nanostructures [3].

The unique properties possessed by magnetic nanoparticles depend on their chemical content and microstructure characteristics, where the microstructure such as particle shape and size can be controlled through the process of synthesis of the material. Many methods have been developed in the synthesis of nanoparticles such as the sonochemical method [4], hydrothermal, sol-gel, auto-combustion [5-6], thermal decomposition, solvothermal method, co-precipitation [7-8], microwave, micro-emulsion, electrochemical, laser ablation, and mechanical milling [9]. Among these methods, the co-

precipitation method is the most promising method due to the easy process and can produce relatively small particle size distributions on the resulting material. In addition, this method also can be done in normal environmental conditions. By using this method, the crystal structure and magnetic properties can be optimized by controlling the synthesis parameters such as temperature, solvent, pH of the solution, stirring speed, stirring time, metal salt concentration, co-precipitant concentration, and surfactant concentration.

Along with modified materials by the synthesis process, researchers have explored various possibilities of the substitution materials for cobalt ferrite, such as magnesium, zinc, calcium, zirconium, chromium, nickel, and lead. The structure and magnetic properties of ferrite have been observed by adding other material into ferrite nanoparticles, known as dopping. Nickel is one of the good materials as doping. By substituting the nickel into the cobalt ferrite, the coercivity and saturation magnetization was decreased due to their magnetocrystalline anisotropy and magnetic moments. Cobalt Nickel Ferrite ($CoNiFe_2O_4$) showed high resistivity and good magnetic properties. Therefore, through this paper, we have investigated the effect of variation of concentration Ni^{2+} as substitute material on structure and magnetic properties of $CoFe_2O_4$ by the co-precipitation method. The raw material used was natural iron sand of Jeneberang River, Sulawesi as a source of Fe ions. The natural iron sand was chosen because it has an abundant amount. The result samples were characterized using X-Ray Diffraction (XRD) to analyses the structure and crystal phase of materials. The analysis of the magnetic properties of materials was also conducted by the Vibrating Sample Magnetometer (VSM).

2. EXPERIMENTAL

Nanoparticle $Co_{1-x}Ni_xFe_2O_4$ was synthesized using the co-precipitation method. We used the natural iron sand of Jeneberang River as the main precursors which provide Fe^{3+} ions. The other chemical precursors such as $NiCl_2.6H_2O$ and $CoCl_2.6H2O$ as a provider of Ni^{2+}/Co^{2+} ion with a coefficient ratio of 1:2. The synthesis process was carried out by dissolving 16 grams of iron sand into 50 mL HCl solution (37%) and stirring for 30 minutes. Furthermore, $NiCl_2.6H_2O$ and $CoCl_2.6H_2O$ have dissolved into 10 mL aquadest. Then, the Fe^{3+} solution was mixed with the Ni^{2+}/Co^{2+} solution until the homogeneous was obtained. The mixture solution marked as a cationic solution. After that, the cationic solution added dropwise into 150 mL of NaOH solution (4 M) while stirring using a magnetic stirrer at stirring speed 350 rpm for 2 hours at temperature 70 ºC. The synthesis parameters can be seen in Table 1.

The formed solution was placed on a magnetic stirrer to speed up the decomposition process. Then the sediment was washed using aquadest several times to remove the excess of salt and any impurities. This step was needed in order to increase the purity of sample $Co_{1-x}Ni_xFe_2O_4$ which will be obtained. Furthermore, the sample was centrifuged at 2000 rpm for 10 minutes to

separate the sediment with an excess of water. To obtain $Co_{1-x}Ni_xFe_2O_4$ powder, then the sediment is dried in oven at temperature 80° C. After that, the dried sample was crushed using hand mortar, and the powder further was sintered at a temperature of 600 °C for 1 hour.

Table.1. Parameters synthesis of nanoparticles $Co_{1-x}Ni_xFe_2O_4$ various mole concentration of Ni^{2+}

Sample	Mass of iron sand (g)	Mass $CoCl_2.6H_2O$ (g)	Mass $NiCl_2.6H_2O$ (g)	HCl 37% volume (mL)	NaOH concentration (M)	Duration of stirring (minute)	Synthesis temperature (°C)
$CoFe_2O_4$	16	8.9212	0	50	4	120	70
$Co_{0.75}Ni_{0.25}Fe_2O_4$	16	6.6757	1.8802	50	4	120	70
$Co_{0.50}Ni_{0.50}Fe_2O_4$	16	4.4618	3.7326	50	4	120	70
$Co_{0.25}Ni_{0.75}Fe_2O_4$	16	2.2160	5.6404	50	4	120	70

$Co_{1-x}Ni_xFe_2O_4$ powders with various concentrations of Ni^{2+} that had obtained were characterized by X-Ray Diffraction (Rigaku Smartlab, wavelength λ = 1,541862 Å) to determine the phase of materials. The crystallite size distribution is determined by the expansion of the main peak of XRD results using the Debye-Scherrer equation, which is written as [10]:

$$D = \frac{k\lambda}{\beta \cos\theta} \qquad (1)$$

where, k is the Scherer constant (0,89), λ is the wavelength of X-ray and β is the width of half the peak FWHM (*full width at half maximum*) of the main peak. The lattice parameter in the sample is calculated in equation 2 as shown below [11],

$$a = \frac{\lambda\sqrt{h^2+k^2+l^2}}{2\sin\theta} \qquad (2)$$

where (h k l) are the Miller indices and θ is the diffraction angle according to the (h k l). To the defect in density crystal and lattice voltage are calculated using equation [12-13]:

$$\delta = \frac{1}{D^2} \qquad (3)$$

$$\varepsilon = \frac{\beta}{4\tan\theta} \qquad (4)$$

where, δ is the dislocation density and ε is the lattice strain. Meanwhile, to find out the unit cell volume, crystal volume and number of cells for ferrite spinel is calculated using the following equation [14]:

$$V_{cell} = a^3 \qquad (5)$$

$$V_{crys} = \frac{4}{3}\pi\left(\frac{D}{2}\right)^2 \qquad (6)$$

$$S = \frac{V_{crys}}{V_{cell}} \qquad (7)$$

The magnetic properties of sample was investigated using the *Vibrating Sample Magnetometer* (VSM) (VSM 250 Dexing Co.Ltd.). The results from the VSM measurements are the calculated to get the value of the magnetic moment with the following equation [15]:

$$\eta_\beta = \frac{M.M_s}{5585} \qquad (8)$$

where η_β is magnetic moment, Ms is saturation magnetization, M is molecular weight and 5585 is a magnetic factor.

3. RESULTS AND DISCUSSION

A. *Structural Properties*

The *X-Ray Diffraction* (XRD) analysis was conducted to study the crystallographic of the transition metal nanostructured ferrite. This XRD analysis result provided information about crystal structure, orientation, and average crystal size. In Figure 1 shows the XRD patterns of $Co_{1-x}Ni_xFe_2O_4$ nanoparticles. The patterns indicated that the formation of $Co_{1-x}Ni_xFe_2O_4$ phase with a cubic spinel structure with a peak diffraction corresponding to crystalline planes of (220),

(311), (400), (422), (511), and (440). It also can be seen that no impurity phase was detected in all samples, which means the $Co_{1-x}Ni_xFe_2O_4$ nanoparticles formed are all single phase with strong intensity confirmed. The XRD results can also be used to estimate the lattice parameters and crystallite size of the samples. The lattice parameter can be evaluated using the Bragg Law equation in equation (2) and the crystallite size can be calculated using equation (1) based on the full width value (FWHM) at the maximum half of the plane peak (311) which is the main peak in the XRD patterns.
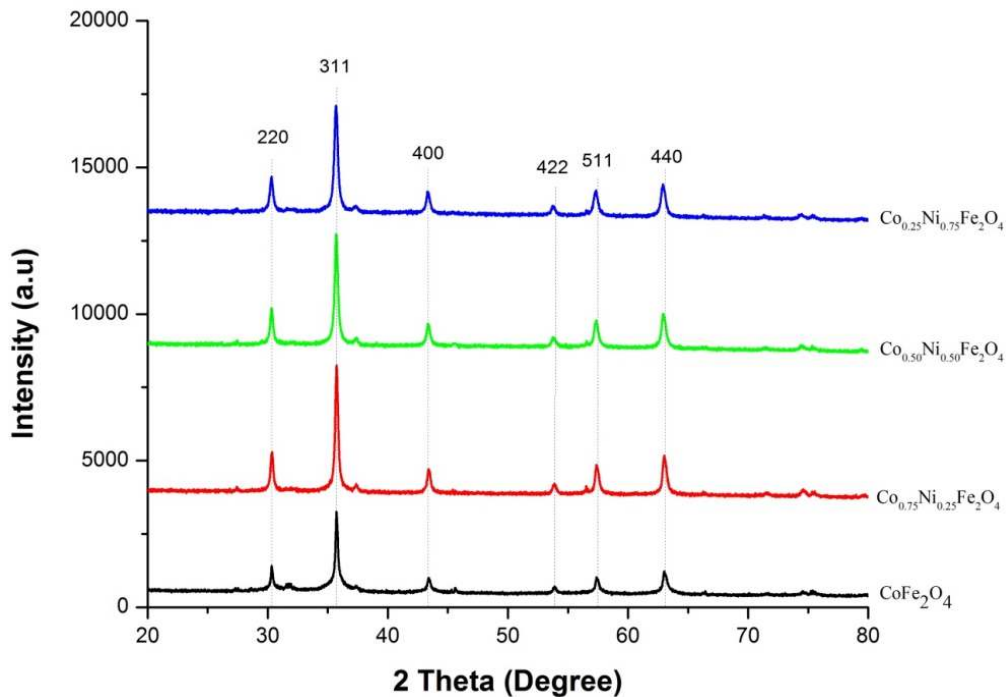
Figure 1. X-ray Diffraction (XRD) curves of $Co_{1-x}Ni_xFe_2O_4$ nanoparticles with various concentrations of Ni^{2+}

Table.2. The lattice parameter of $Co_{1-x}Ni_xFe_2O_4$ samples based on the XRD results

Sampel	a(Å)	D (nm)	δ ($\times10^{15}$ line/m^2)	ε ($\times10^{-3}$)	V_{cell} ($\times10^{-1}$ m^3)	V_{crys} ($\times10^3$ m^3)	S ($\times10^3$)
$CoFe_2O_4$	8.334	56.55	0.31	1.97	5.78	94.76	16.36
$Co_{0.75}Ni_{0.25}Fe_2O_4$	8.336	33.84	0.87	3.30	5.79	20.30	3.50
$Co_{0.50}Ni_{0.50}Fe_2O_4$	8.342	30.24	1.09	3.70	5.80	14.49	2.49
$Co_{0.25}Ni_{0.75}Fe_2O_4$	8.348	25.96	1.48	4.31	5.81	9.16	1.57

The analysis of the XRD such as lattice parameter (a), crystallite size (D), dislocation density (δ), lattice strain (ε), the volume of cell unit (Vcell), the volume of crystallite (Vcrys) and a number of cells (S) have been calculated for each sample presented in Table 2, which shows that by increasing the concentrations of Ni^{2+}, the peak shifted slightly to a low 2θ angle and the lattice parameter increases from a=8.334 Å for $CoFe_2O_4$ (x=0) to a=8.348 Å for $Co_{0.25}Ni_{0.75}Fe_2O_4$ (x=0,75). The increased lattice parameters caused by differences in the radius of the Co^{2+} (0.78) and Ni^{2+} (0.69) atoms. However, there is no linear dependence of the lattice parameters on samples synthesized with variations of Ni^{2+}. This may occur due to the relevant defects in the magnetic nanostructure, such as lattice deformations, oxygen voids, and lengths. Moreover, the crystallite size of the samples was obtained about 25.96-56.55 nm as shown in Table 2. This shows that the size of crystallite gradually decreased with increasing concentrations of Ni^{2+} which is predicted to occur as Ni^{2+} can affect the rate of nucleation and growth of crystals by accelerating the rate of nucleation and slowing the crystal growth. In addition, Ni^{2+} ions are more difficult to substitute into the spinel structure compared to Co^{2+} ions, thereby the addition of Ni^{2+} which substitutes Co^{2+} causes decreased or inhibited crystal growth activity of nanoparticles during the synthesis process. Previous studies was confirmed in our present studies [16-18]. Table 2 also shows that to arrangement irregularities of the crystals such as dislocation density and lattice strain tends to be greater as the presences of Ni^{2+} in the sample, while the volume of crystal and volume of cell number is getting smaller. This is due to a large amount of Ni^{2+} which substitutes Co^{2+} which can cause smaller crystallite sizes.

B. Magnetic Properties

The magnetic properties of the $Co_{1-x}Ni_xFe_2O_4$ nanoparticles were determined using a VSM (*Vibrating Sample Magnetometer*) which runs at room temperature. The hysteresis curve of samples was shown in Figure 2. The hysteresis shows that all samples are typical ferromagnetic with different coercivity values (Hc). The values of saturation magnetization (Ms), remanence magnetization (Mr) and coercivity (Hc) for various variations of Ni^{2+} concentration have been inserted in Table 3. It can be seen that the smaller the crystal size, the coercivity value tends to be smaller and vice versa. However, in the sample of $Co_{0.25}Ni_{0.75}Fe_2O_4$, there was slightly an increase of coercivity which was thought to be due to the agglomeration. The decrease of coercivity by an increase of Ni^{2+} concentration can be attributed to the lower magneto-crystalline anisotropy of Ni^{2+} ions compared to Co^{2+} ions which lead to lower coercivity of $CoFe_2O_4$ (cobalt ferrite). Thus, the smaller the crystal size, there is a decrease in the barrier energy (anisotropy energy) in the particle. So that the magnetic moment in the sample will be easily magnetized by an external magnetic field and when demagnetized the coercivity will tend to be smaller. The decreased coercivity and tends to zero at x = 0 indicates that the sample gradually

tends to exhibit super-paramagnetic properties with increasing concentrations of Ni^{2+}.

Figure 2 shows the hysteresis curves of substituted Cobalt Nickel Ferrite (Co1-xNixFe2O4 for various x values) at room temperature. The saturation magnetization observed to decrease with increasing nickel concentration from 35,811 emu/grams to 23,42 emu/grams. The downward trend in magnetization has also been reported by others. According to Kim & Shima (2007), there are two possible models that can explain the decrease in Ms when the Ni^{2+} content increases, namely the surface rotational disturbance model and the uniformly reduced magnetic moment model [19]. However, for $Co_{1-x}Ni_xFe_2O_4$ nanoparticles, the decrease of Ms due to the higher magnetic moment at Co^{2+} than Ni^{2+} at the octahedral site in an inverted spinel structure [20]. In $Co_{1-x}Ni_xFe_2O_4$ samples, Ni^{2+} ions are on the octahedral site while Co^{2+} and Fe^{3+} ions occupy the tetrahedral and octahedral sites. This phenomenon can be explained by the redistribution of tetrahedral and octahedral sites and changes in exchange interactions between tetrahedral and octahedral sublattices.

The area of the hysteresis curves in a sample can shows the amount of energy of magnetization, thus in Figure 2 it can be seen that $CoFe_2O_4$ requires greater magnetization energy compared to other samples. Due to the crystallite size in the sample is much larger than in other samples as the Co^{2+} content increases, the amount of domain increase as well. By increasing the number of domains, thus requires a lot of energy compared to sample which has a few domains [21].
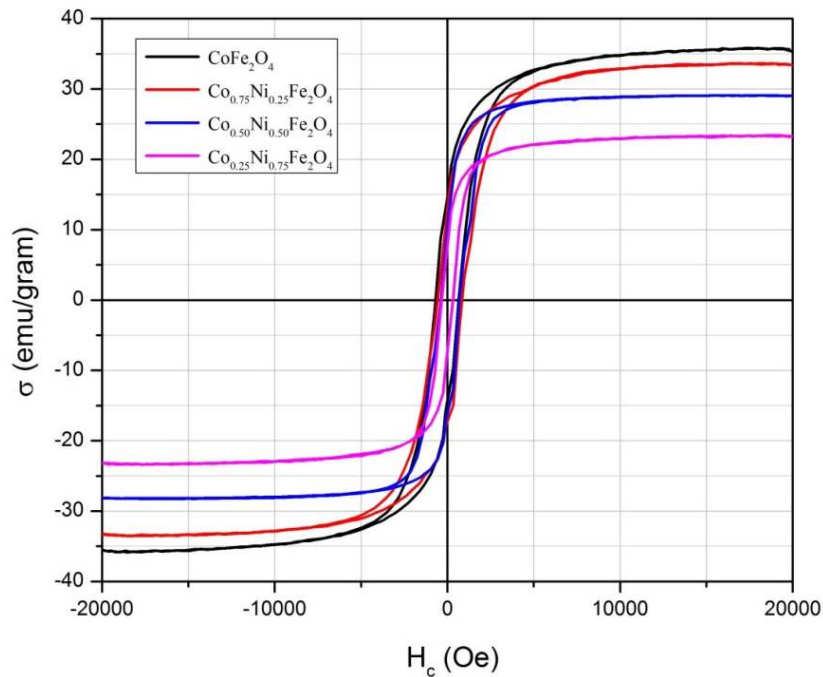
Figure.2. Hysteresis curves of $Co_{1-x}Ni_xFe_2O_4$ nanoparticles with varying concentrations of Ni^{2+}

Table.3. Vibrating Sample Magnetometer (VSM) observations in $Co_{1-x}Ni_xFe_2O_4$ samples

Sample	D (nm)	H_c (Oe)	M_s (emu/gram)	M_r (emu/gram)	η_b (emu/mol)
$CoFe_2O_4$	56.55	663.95	35.81	14.36	1.74
$Co_{0.75}Ni_{0.25}Fe_2O_4$	33.84	471.66	33.65	12.52	1.63
$Co_{0.50}Ni_{0.50}Fe_2O_4$	30.24	298.20	29.07	10.04	1.41
$Co_{0.25}Ni_{0.75}Fe_2O_4$	25.96	319.89	23.42	7.67	1.14

4. CONCLUSIONS

The synthesis using co-precipitation has been able to produce $Co_{1-x}Ni_xFe_2O_4$ nanoparticles by substituting Ni^{2+} into $CoFe_2O_4$. The result obtained that the lattice parameter increase by increasing of Ni^{2+} ions so that the crystallite size tends to be smaller. The coercivity as well as crystallite size tend to decrease by increasing Ni^{2+}. However, on a sample $Co_{0.25}Ni_{0.75}Fe_2O_4$ coercivity values increased. This happens allegedly due to agglomeration of the sample. Based on the magnetic properties analysis, it shows that when the crystallite size gets smaller, the coercivity also decreases which indicates the magnetic properties change from ferromagnetic to soft magnetic properties. The analysis of magnetization shows that saturation and remanence magnetization values tend to be smaller along with the increasing Ni^{2+} content.

REFERENCES

[1] Parishani, M., Cheragi, A., and Malekfar. R., 2015. International Journal of Optics and Photonics (IJOP) **9** 73-78

[2] Setiadi, E. A., Yunus, M., Nababan, N., Simbolon, S., Kurniawan, C., Humaidi, S., Sebayang, P., and Ginting, M., 2018. *J. Phys.: Conf. Ser* **985** 012046

[3] Chand, P., Vaish, A., and Kumar, P., 2017. Physica B. **524:** 53-63

[4] Almessiere, M. A., Slimani, Y., Guner, S., Sertkol, M., Demir, K. A., and Sagar, E., Shirsath. 2019. Ultrasonics-Sonochemistry **58** 104654

[5] Uday, B. S., Narsinga, R. G., Chou, F. C., and Ramana, R. M. V., 2018. Journal of Magnetism and Magnetic Materials. **452:** 398-406

[6] Hakare, P. P., Sanadi, K. R., Garadkar, K. M., Pati, D. R., and Mulia, I. S., 2013. Journal of Alloys and Compounds. **553:** 383-388

[7] Sari, A. Y., Eko, A. S., Candra. K., Hasibuan, D. P., Ginting, M., Sebayang, P. and Simamora, P., 2017. IOP Conf. Ser.: Mater. Sci. Eng **214** 012021

[8] Setiadi, E. A., Simbolon, S., Rahmat, Yunus, M., Kurniawan, C., Tetuko, A. P., Zelviani, S., Rahmaniah and Sebayang, P., 2018. J. Phys.: Conf. Ser **979** 012064

[9] Kebede, K., Kefeni, Tinus A. M., Msagati and Bhekie B. M., 2017. Materials Science and Engineering B **215** : 37-55

[10] Zaheer, H. S. S., Khan, U., Riaz, S., and Naseem. S., 2015. Material Today **2** : 5214-5219

[11] Pahadatare, M. R., 2013. Journal of Alloys and Compounds **546**: 314-319.

[12] Setiadi, E. A., Amriani, F., and Sebayang, P., 2017. AIP Conference Proceedings **1904** 020039

[13] Mimouni, R., Kamoun, O., Yumak, A., Mhamdi, A., Boubaker, K., Petkova, P., and Ambuk, M., 2015. Journal of Alloys and Compounds. **654**: 100-111

[14] Singh, A, et al., 2014. Mater. Sci. Semicond. Process **27**:934-949

[15] Ghodake, U. R., Chaudhari, N. D., Kambale, R. C., Patil, J. Y. and Suryavanshi, S. A., 2016. Journal of Magnetism and Magnetic Materials **407**:60-68

[16] Juang, X., Yanqiu. C., Xiangqian, S., Guangzhen, Z., and Yintao, G., 2012. Journal of Colloid and Interface Science. **376**:57-61

[17] Maaz, K., Khalid, W., Mmtaz, A., Hasanain, S. A., Liu, J. and Duan, J. I., 2009. Physica E **41**;593-599

[18] Salazar-Kuri, U., Estevez, J. O, Silva-Gonzalez, N. R., Pal, U., and Mendoza, M. E., 2017. Journal of Magnetism and Magnetic materials **442**:247-254.

[19] Kim, T. and Shima, M., 2007. Journal of Applied Physics **101** 09M516

[20] Qi, Y. I., Yang, Y. X., and Zhao, X. F., 2010. Particunology **8**:207-211

[21] Taib, S. and Suharyadi, E., 2015. Indonessian Journal of Applied Physics **5**:23